The Progression of Muscle Fatigue During Exercise Estimation With the Aid of High-Frequency Component Parameters Derived From Ensemble Empirical Mode Decomposition

Shing-Hong Liu, Kang-Ming Chang, and Da-Chuan Cheng

***Abstract*—Muscle fatigue is often monitored via the median frequency derived from the surface electromyography (sEMG) power spectrum during isometric contractions. The power spectrum of sEMG shifting toward lower frequencies can be used to quantify the electromanifestation of muscle fatigue. The dynamic sEMG belongs to a nonstationary signal, which will be affected by the electrode moving, the shift of the muscle, and the change of innervation zone. The goal of this study is to find a more sensitive and stable method in order to sense the progression of muscle fatigue in the local muscle during exercise in healthy people. Five male and five female volunteers participated. Each subject was asked to run on a multifunctional pedaled elliptical trainer for about 30 min, twice a week, and was recorded a total of six times. Three decomposed methods, discrete wavelet transform (DWT), empirical mode decomposition (EMD), and ensemble EMD (EEMD), were used to sense the progression of muscle fatigue. They compared with each other. Although the highest frequency components of sEMG by DWT, EMD, and EEMD have the better performance to sense the progression of muscle fatigue than the raw sEMG, the EEMD has the best performance to reduce nonstationary characteristics and noise of the dynamic sEMG.**

***Index Terms*—Discrete wavelet transform (DWT), empirical mode decomposition (EMD), ensemble EMD (EEMD), median frequency (MF), muscle fatigue.**

I. Introduction

PEOPLE use sport equipment to train their body for health improvement. The sports equipment includes the treadmill, elliptical trainer, and bike. Moreover, isokinetic exercise using these equipment has been widely applied for functional rehabilitation and assessment [1], [2], as isokinetic tests have been proven helpful in acquiring a better comprehension of the biomechanics in the lower limb muscles during dynamic contractions [3], [4]. However, how to develop an appropriate exercise is an important issue in healthy and pathological subjects.

Muscle fatigue is defined as a loss of the required or expected force from a muscle, and has been an attractive research issue for a long time. The nature of muscle fatigue and its relation to muscle activity have been studied [5]. It is well known that the power spectrum of the surface electromyography (sEMG) is toward the lower frequency during a sustained muscle contraction. At this time, the spectral parameters, such as the mean frequency (MNF) and the median frequency (MF), are the electrical manifestation of localized muscle fatigue [6], [7]. According to most reports that studied muscle fatigue, the changes in muscle fiber propagation velocity and the firing rate of muscle fibers could affect the sEMG power spectrum [8]–[12]. In an isometric and sustained muscle contraction, the sEMG may be assumed as a wide-sense stationary signal, and thus, its power spectrum could be obtained using common spectral estimation techniques. Although the activity of sustained muscle contraction is often satisfactory in rehabilitation medicine and ergonomics, the exercises are often the dynamic most of the time. In this case, signals are nonstationary, and therefore, appropriate spectral estimation techniques are required.

In many studies, the sEMG has been considered a realization of a nonstationary stochastic process [11], and the shift of the innervation zone always happens during a dynamic contraction [12]. Therefore, Molinari *et al.* [13], [14] proposed signal processing methods to assess the spectral changes of sEMG due to fatigue during dynamic contraction. Dingwell *et al.* [15] quantified both localized muscle fatigue and movement kinematics change over time during exhaustive cycling. Tscharner [16] used the wavelet analyses to estimate the sEMG parameters during a mildly fatiguing exercise on a cycle ergometer. In these research groups, they always used the measurement system of multiple channels and the complex analyzed method to quantify the electrical manifestations of muscle fatigue for the pathological subjects. However, using a single-channel sEMG and a nonstationary signal process to sense the progression of muscle fatigue for the exercise of health people could be easily applied in health care. Some nonlinear approaches are also very

Manuscript received May 19, 2013; revised August 21, 2013; accepted October 14, 2013. Date of current version September 2, 2014. This work was supported in part by the National Science Council of Taiwan under Grants NSC 102–2221-E-324 -004 and NSC 102–2221-E-468–003. *(Correspondig author: K.-M. Chang.)*

S.-H. Liu is with the Department of Computer Science and Information Engineering, Chaoyang University of Technology, Taichung 41354, Taiwan (e-mail: shliu@cyut.edu.tw).

K.-M. Chang is with the Department of Photonics and Communication Engineering, Asia University, Taichung 41354, Taiwan. He is also with Graduate Institute of Clinical Medical Science, China Medical University, Taichung, Taiwan (e-mail: changkm@asia.edu.tw).

D.-C. Cheng is with the Department of Biomedical Imaging and Radiological Science, China Medical University, Taichung 404, Taiwan (e-mail: dccheng@mail.cmu.edu.tw).

Color versions of one or more of the figures in this paper are available online at http://ieeexplore.ieee.org.

Digital Object Identifier 10.1109/JBHI.2013.2286408

attractive methods to evaluate muscle fatigue on sEMG, such as Lempel–Ziv complexity measure [17] and Fuzzy approximate entropy [18]. González-Izal *et al.* have reviewed the linear and nonlinear sEMG models for estimating muscle fatigue [19].

Recently, a useful nonstationary and nonlinear signal processing technique, known as empirical mode decomposition (EMD), has been proposed. EMD was introduced by Huang, and has been widely used for nonlinear signal analysis [20]. The principle of EMD is based on a decomposition derived from the data, and is useful in the analysis of nonlinear and nonstationary time-series signals. With an iterative decomposition of signals, EMD separates the full signal into ordered elements with frequencies ranging from high to low in each intrinsic mode function (IMF) level. The filter bank-like property of EMD has been widely applied in biomedical signal analysis [21], [22]. The decomposed IMFs were further extracted with the power or entropy approach to analyze the nonstationary biosignals for noise reduction and for feature extraction. Srhoj *et al.* have extracted the MF from selected IMFs of sEMG recorded over the quadriceps muscles during cyclic dynamic contractions [23]. Their results showed that HHT-derived spectral and linear regression parameters were consistent and more reliable than those obtained with the short-time Fourier transform and the wavelet transform.

The newly developed ensemble EMD (EEMD) has improved the mode mixing effect of adjacent IMF functions, which is the main disadvantage of EMD [24]. Mode mixing indicates that oscillations of different time scales coexist in a given IMF or that oscillations with the same time scale have been assigned to different IMFs. The procedure of the EEMD is to add statistically zero-mean noise into the signal with sufficient trials, and the ensemble IMF is estimated by the summation of the IMF from each trial of the same level.

The goal of this study is not to quantify the myoelectric manifestation of muscle fatigue. Our goal is to find a more sensitive and stable method to sense the progression of muscle fatigue in the local muscle during exercise in healthy people. We used a self-designed wireless apparatus to record the sEMG signal of the vastus lateralis in the left leg of each volunteer. There were ten healthy volunteers who joined this experiment; they ran in a multifunctional pedaled elliptical trainer. Each subject performed six experiments in three weeks. We hypothesized that healthy subjects run a fixed speed with different loads in muscle activity as fatigue progressed. We also hypothesized that its spectral parameters will have a significant change during the dynamic contraction when the decomposed signal of sEMG reduced the nonstationary characteristics and noise.

II. Methods

A. Wireless Measurement Apparatus

A wireless measurement apparatus was developed by the authors at a size of 5.7 cm × 4.3 cm, with the distance of the electrodes 3.6 cm, as shown in Fig. 1. The gain of the device is 1000. A two-order high-pass filter was used to reduce the baseline with a cutoff frequency of 30 Hz. A two-order low-pass filter was used as the antialiasing filter with a cutoff frequency of 1000 Hz. This device is based on the microcontroller MSP430-F5342 as the core structure, which has a 12-bit analog-to-digital converter with a sampling rate of 2000 Hz. The digital EMG signal is transferred by a Bluetooth chip to a remote server. A visual basic-based interface system was used to display and store the digital EMG data in real time.

Fig. 1. Real photo of the wireless measurement apparatus: (a) the front view and (b) the back view.

TABLE I
Subject Characteristics

Variable	Male (n=5)	Female (n=5)
Age (years)	24 (2)	21 (2)
Weight (kg)	78.6 (10.8)	53.3 (5.3)
Height (cm)	176.5 (6.8)	163.6 (4.7)
BMI (kg/m^2)	25.0 (3.9)	19.8 (1.4)

Data are expressed as the mean (standard derivation). BMI is the body mass index.

Fig. 2. Illustration of the wireless measurement apparatus worn on the left vastus lateralis.

B. Subjects and EMG Recording

There were ten volunteers involved (five male and five female), with ages ranging from 19 to 27 years. Their information is listed in Table I. The participants were required to run in a multifunctional pedaled elliptical trainer (Johnson E8000). We measured the vastus lateralis of the left leg, as shown in Fig. 2. According to [25], EMG studies on the trapezius, vastus medialis, and lateralis muscles dips and plateau regions related to the presence of innervation zone. Thus, we avoided the belly position and shifted the electrodes to a higher position. The surface electrodes used for the EMG recording were Ag/AgCl with a 10-mm diameter on self-adhesive supports. The electrode arrangement ensured negligible crosstalk between adjacent muscles. The positions of the electrodes for each subject were recorded, and the electrodes were placed at the same position in the subsequent experiments.

C. Experimental Procedure

The muscle fatigue experiment is based on the following procedures.

Step 1: The subjects are required to wear the wireless sEMG device. Alcohol is used to clean the surface, and electrolytic gel is smeared on the electrodes to decrease the contact impedance. Athletic tape is used to fix the apparatus, and thus, avoid movement of the electrodes. Before data collection, a consent form was signed by each subject.

Step 2: There are three load levels in the multifunctional pedaled elliptical trainer, $L2$, $L4$ and $L6$, with $L2$ being light and $L6$ being heavy. The speed range of $L2$ is 55–60 steps per minute (SPM) for males and 50–55 SPM for females. The speed range of $L4$ is 60–70 SPM for males and 55–65 SPM for females. The subjects are required to run at their maximum speed until exhaustion for $L6$, which has a faster speed range than $L4$. The speed range is 80–100 SPM for males and 70–90 SPM for females. A 10-min session is required for both $L2$ and $L4$. In the pre-experiment, the subjects tested the speed range and chose the most appropriate speeds for the $L2$ and $L4$ levels, separately. These speeds were recorded for every participant. In the experiments, the subjects ran at their self-selected speeds during the experimental procedure.

Step 3: In order to avoid the training phenomenon, each subject was only recorded twice a week at the same time, and the rest time must be more than two days. There were a total of six recording times for each subject.

D. EMD and EEMD Algorithm

The EMD algorithm used in this study comprised the following steps [20] and demonstrated in Fig. 3(a).

Step 1: Extrema (maxima and minima) of the signal, *x(t)*, are identified.

Step 2: Upper and lower envelopes of the extreme point are developed.

Step 3: Mean function of the upper and lower envelopes, *m(t)*.

Step 4: Difference signal $d(t) = x(t)–m(t)$.

Step 5: If $d(t)$ becomes a zero-mean process, then the iteration stops, and $d(t)$ is a first IMF (IMF1), called $c_1(t)$; otherwise, go to Step 1 and replace $x(t)$ with $d(t)$.

Step 6: Residue signal $r(t) = x(t)-c_1(t)$.

Step 7: Replace *x(t)* with *r(t)* and repeat the procedure from Steps 1 to 6 to obtain the second IMF (IMF 2), called $c_2(t)$. To obtain $c_n(t)$, continue Steps 1 to 6 after n iterations. The process is stopped when the final residual signal *r(t)* is obtained as a monotonic function.

Now, the original signal can be represented as follows:

$$x(t) = \sum_{i=1}^{n} c_i(t) + r(t). \tag{1}$$

Often, we can regard $r(t)$ as $c_n+_1(t)$.

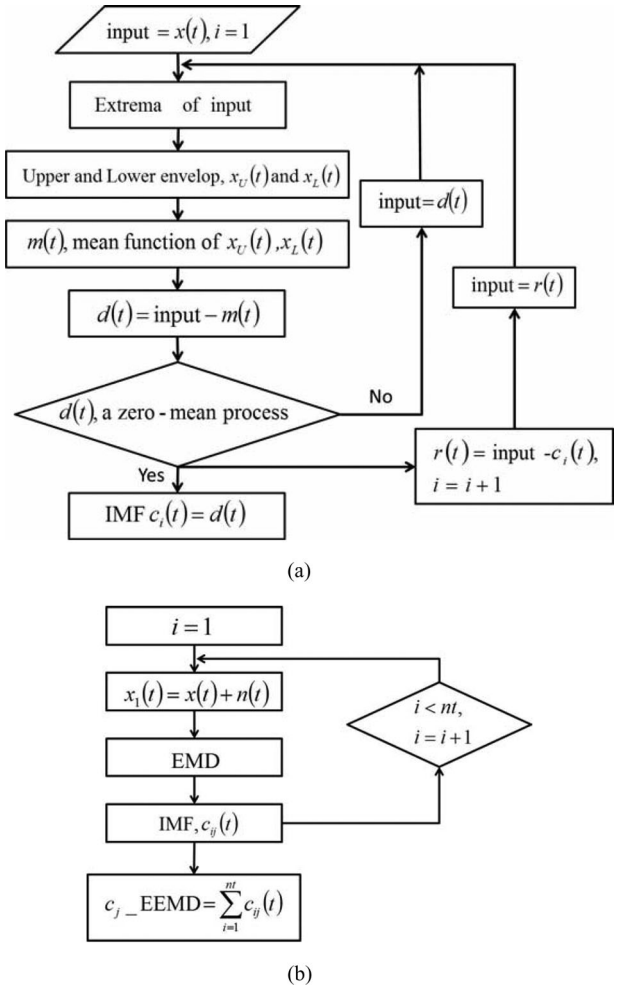

Fig. 3. (a) Flowchart of EMD decomposition. (b) Flowchart of EEMD decomposition.

The EEMD algorithm is as follows [24], and demonstrated in Fig. 3(b).

Step 1: The white noise series *n(t)* was added to the targeted signal *x(t)*, and $x_1(t) = x(t)+n(t)$.

Step 2: Decompose $x_1(t)$ by the standard EMD procedure.

Step 3: Repeat Steps 1 and 2 until the preset number of trial has been completed. Each repeated time was added to the white noise series of the same power at each time for the EMD calculation. The new IMF combination $c_{ij}(t)$ is achieved, where i is the iteration number and j is the IMF scale.

Step 4: Estimate the mean (ensemble) of the final IMF of the decompositions as the desired output:

$$c_j\_\text{EEMD}\,(t) = \sum_{i=1}^{nt} c_{ij}\,(t) \tag{2}$$

where *nt* denotes the total number of trials. In this study, the EMD and EEMD decompositions were estimated using the visual signal software. The number of trials is 100, and the added noise power is 14 dB. The order of the IMF is 20 and 21 for EMD and EEMD,

respectively. The calculated EMD- and EEMD-based IMFs were used for further muscle fatigue analysis in Matlab R2010.

E. Discrete Wavelet Analysis

Assuming the raw sEMG signal is $x[n]$, the discrete wavelet transform (DWT) decomposition involves the following filtering process:

$$A_j[n] = \sum_{k=-\infty}^{\infty} A_{j-1}[k] \cdot h[2n-k] \tag{3}$$

$$D_j[n] = \sum_{k=-\infty}^{\infty} A_{j-1}[k] \cdot g[2n-k] \tag{4}$$

where $A_0[n] = x[n]$ and $A_j[n]$ and $D_j[n]$ indicate the coarse and detailed sequences, respectively, after the jth decomposition. The variable $h[n]$ represents the half-band low-pass filter, and $g[n]$ represents the half-band high-pass filter. The original signal is decomposed from the high-frequency component to the low-frequency component as a combination of $A_j[n]$ and $D_j[n]$. For example, if the decomposition level is 5 ($j = 5$), then the original signal can be represented as follows:

$$x[n] = D_1[n] + D_2[n] + D_3[n] + D_4[n] + D_5[n] + A_5[n]. \tag{5}$$

F. Muscle Signal Processing

MNF and MF provide some basic information about the spectrum of signal and its time. But, MF estimates have been shown which are less affected by additive noise and more affect by fatigue [26]. Therefore, we used the MF to sense the progression of muscle fatigue in the local muscle during exercise. Because we have used the hardware filters to reduce the noise, the recorded sEMG or the decomposed signals are directly divided into segments, and fast Fourier transform was used to get the power spectrum density $p(f)$ of a segment. A segment window size is 30 s, and a step size is 15 s. Each segment's MF is extracted from the power spectrum density. The MF is defined as the frequency at which the accumulated spectrum energy is half of the total spectrum energy, as shown in the following equation:

$$\int_0^{\mathrm{MF}} p(f)\, df = \int_{\mathrm{MF}}^{\infty} p(f)\, df = \frac{1}{2}\int_0^{\infty} p(f)\, df. \tag{6}$$

A further linear regression analysis is applied to the MF distribution during the entire exercise in order to quantify manifestations of muscle fatigue. The linear regression equation is defined as follows:

$$y = Ax + b \tag{7}$$

where y is estimated as the MF, x is the time interval, A is the regression slope, and b is the bias. The slope of distribution MF represents the sensitivity for sensing the progression of muscle fatigue. The greater the sensitivity, the smaller the slope [27]. We also used the correlation coefficient (R) to represent the consistency of methods in the progression of muscle fatigue, which is defined as follows:

$$R = \frac{\sum_{i=1}^{n}(x_i - \overline{x})(y_i - \overline{y})}{\sqrt{\sum_{i=1}^{n}(x_i - \overline{x})^2}\sqrt{\sum_{i=1}^{n}(y_i - \overline{y})^2}} \tag{8}$$

where $\bar{x}$ and $\bar{y}$ are the averages of x and y, respectively.

G. Statistics

In this study, the SIGMAPLOT software package was used to conduct the data analysis. Descriptive statistics were applied to subjects' personal information and muscle fatigue parameters (regression slope, A, and correlation coefficient, R). The data were represented as the mean (standard deviation). Statistical testing of the muscle fatigue parameters obtained from the raw data and the different decomposition methods was performed using t-tests. The significance level for the p-value was set at 0.05.

III. Results

Fig. 4 shows the measured sEMG signal (left column) and their spectrum (right column) at the beginning 10 s of three load levels: (a) the load level is $L2$; (b) the load level is $L4$; and (c) the load level is $L6$. Some artificial noises happen at 400 and 800 Hz, which could be interfered by the digital hardware of this apparatus.

DWT, EMD, and EEMD were used to decompose the sEMG signal. The lower IMF and the lower wavelet detail function both correspond to higher frequency components. The sEMG signal of Fig. 4(c) was decomposed by the DWT, and its decomposed signals, D_1, D_2, D_3, D_4, (left column), and their spectrum (right column) are shown in Fig. 5. The decomposed results of EMD and EEMD for the same sEMG signal are shown in Figs. 6 and 7. We only show the first-four IMFs (left column) and their spectrums (right column) to compare the difference with the raw sEMG signal and the decomposed signals of DWT.

Table II shows the analysis results of one experiment for the raw data and the decomposed signals of the other methods for the entire 30-min experiment. The MF slope of the raw sEMG is –0.012 Hz/s. For the DWT decomposition, the absolute MF slope of the first detail component is significantly larger than the rest of the decomposition ($D1$, slope = 0.03 Hz/s). This is also true for EMD and EEMD: the absolute MF slope of the first IMF is significantly larger than that of the other IMFs (IMF1 of EMD, slope = 0.049 Hz/s; IMF1 of EEMD, slope = 0.074 Hz/s). In the following analysis, only the $D1$ component of the DWT and the IMF1 component of the EMD and EEMD were chosen for further MF estimation and regression analysis. The absolute MF slope of the raw data and the highest frequency components of the three methods is EEMD (0.074 Hz/s) > EMD (0.049 Hz/s) > DWT (0.030 Hz/s) > raw EMG (0.012 Hz/s). The MF distributions of the raw data, the $D1$ component of the DWT, and the IMF1 components of the EMD and the EEMD are shown in Fig. 8.

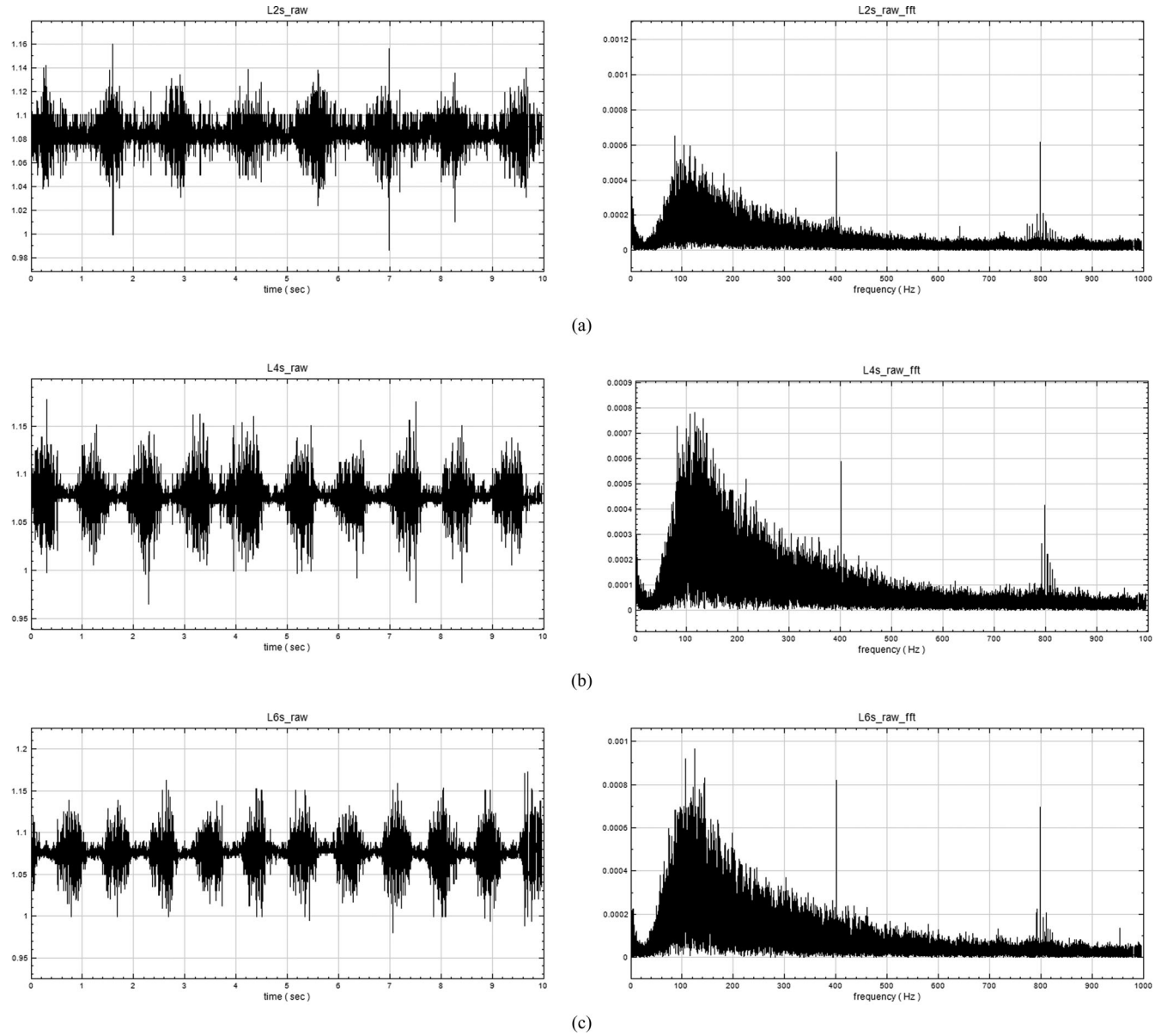

Fig. 4. (Left column) sEMG signal and (right column) their spectrum under three load levels: (a) level $L2$, (b) level $L4$, and (c) level $L6$.

In Table III, the MF slope of the IMF1 component of the EEMD method is significantly different for the raw sEMG signal and the other decomposed methods. The ranges of the absolute MF slope value are EEMD $>$ EMD $>$ DWT $>$ raw sEMG during the three loading levels and the entire exercise. Table IV shows the statistical results of the MF slope of raw data, DWT, EMD, and EEMD at the six measurements. In every measurement, the mean value of the absolute MF slope is also EEMD $>$ EMD $>$ DWT $>$ raw sEMG during the entire exercise. We also used the coefficient of variation, CoV, to show the repeatability of the different methods. Table V shows the statistical results of the slope CoV in the three loading levels and the entire exercise. Although the slope CoV of the EEMD was not significantly different for the raw sEMG signal and the other decomposed methods, the mean and standard deviation were smallest during the entire exercise.

Table VI shows the statistical results of the MF correlation coefficient in the three loading levels and the entire exercise. The MF correlation coefficient for the EEMD method was only significantly different for the raw sEMG signal and the EMD method during the entire exercise. However, the mean of MF correlation coefficient of the EEMD is larger than that of the raw sEMG signal and the other decomposed methods during the entire exercise. Table VII shows the statistical results of correlation coefficient CoV in the three loading levels and the entire exercise. The mean and standard deviation of correlation coefficient CoV of the EEMD are all smallest during the entire exercise.

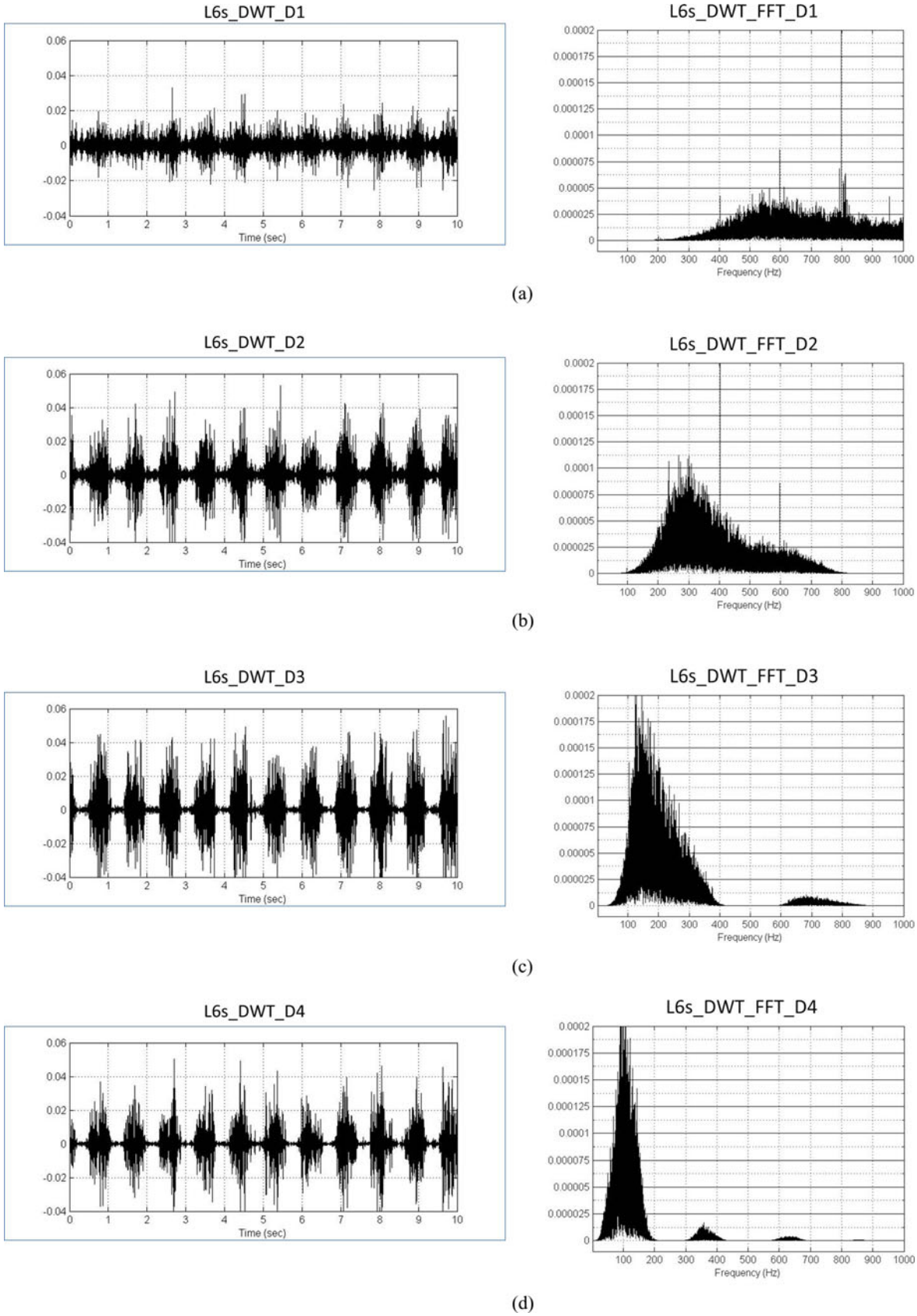

Fig. 5. (Left column) Decomposed sEMG signal and (right column) their spectrum under $L6$ load by the DWT, (a) $D1$ signal, (b) $D2$ signal, (c) $D3$ signal, and (4) $D4$ signal.

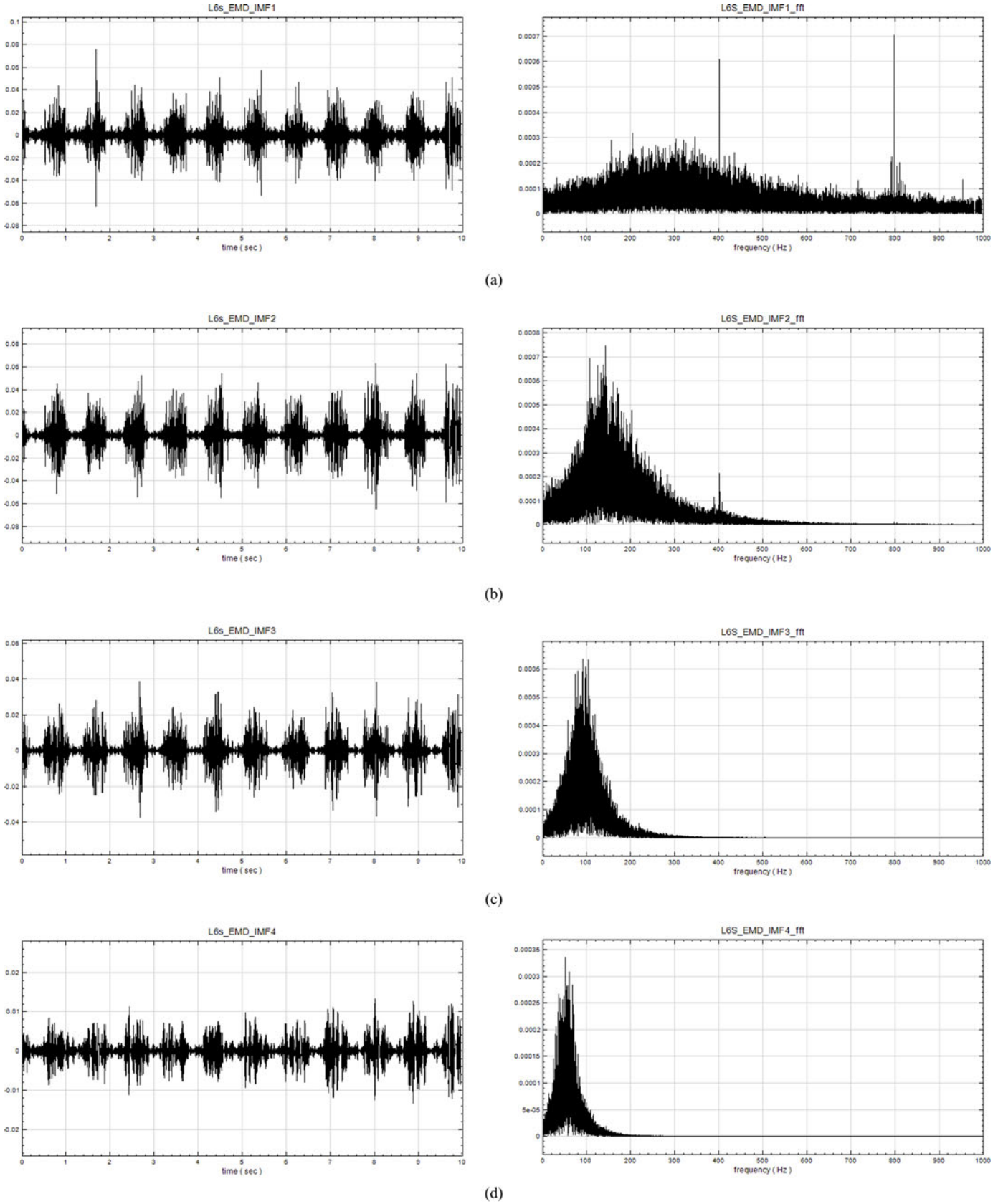

Fig. 6. (Left column) Decomposed sEMG signal and (right column) their spectrum under $L6$ load by the EMD, (a) IMF1 signal, (b) IMF2 signal, (c) IMF3 signal, and (4) IMF4 signal.

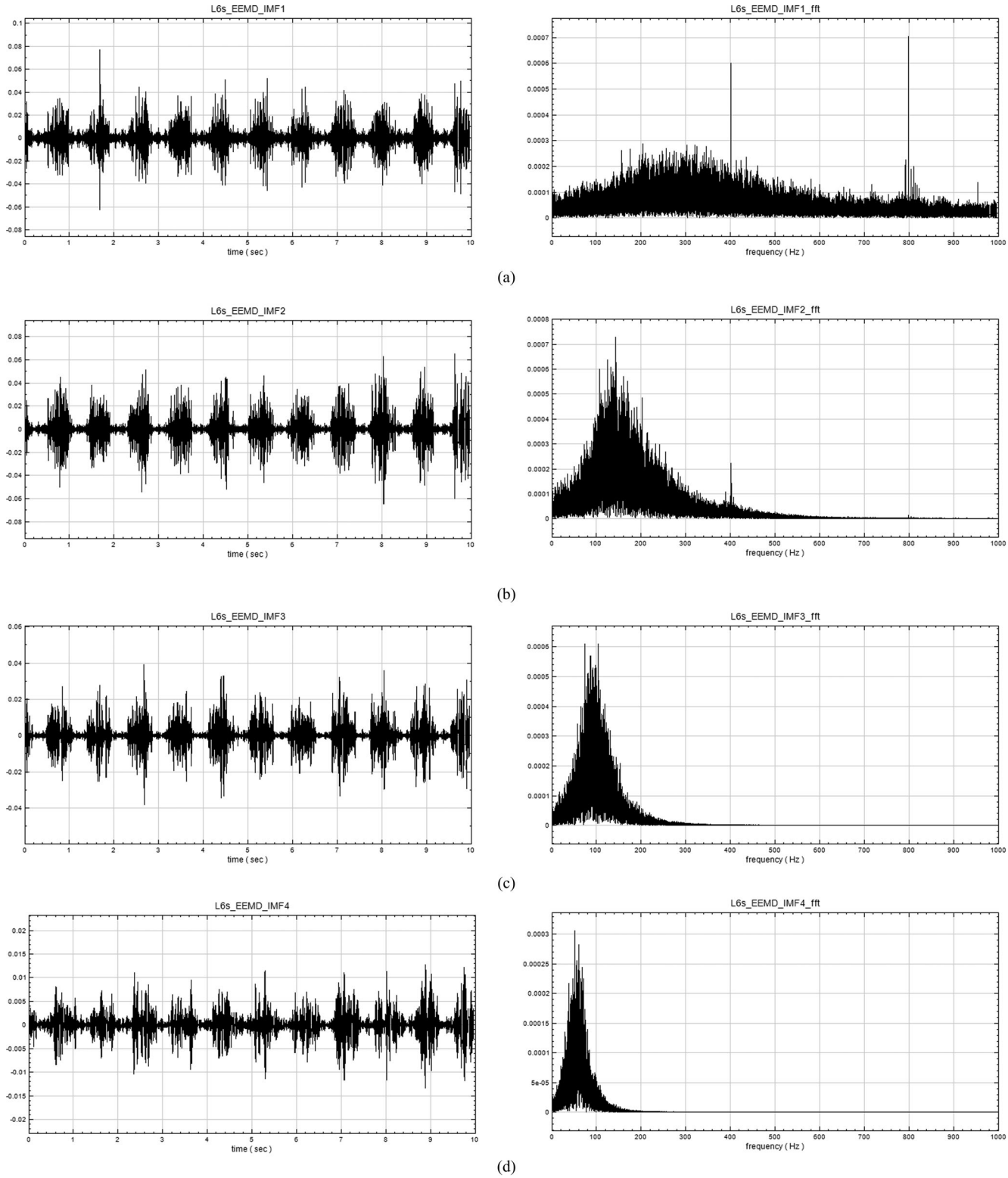

Fig. 7. (Left column) Decomposed sEMG signal and (right column) their spectrum under the $L6$ load by the EEMD, (a) IMF1 signal, (b) IMF2 signal, (c) IMF3 signal, and (4) IMF4 signal.

IV. Discussions and Conclusion

Many other factors affect the results in case of dynamic contractions. One of the main problems is that the sEMG signal may suddenly change their spectral properties when it has the high nonstationarity characteristics. Therefore, some studies used time–frequency analysis methods, such as the short-time Fourier transform [28], the continuous wavelet transform [29], and Choi–Williams distribution (CWD) [13], [14], [30], to evaluate

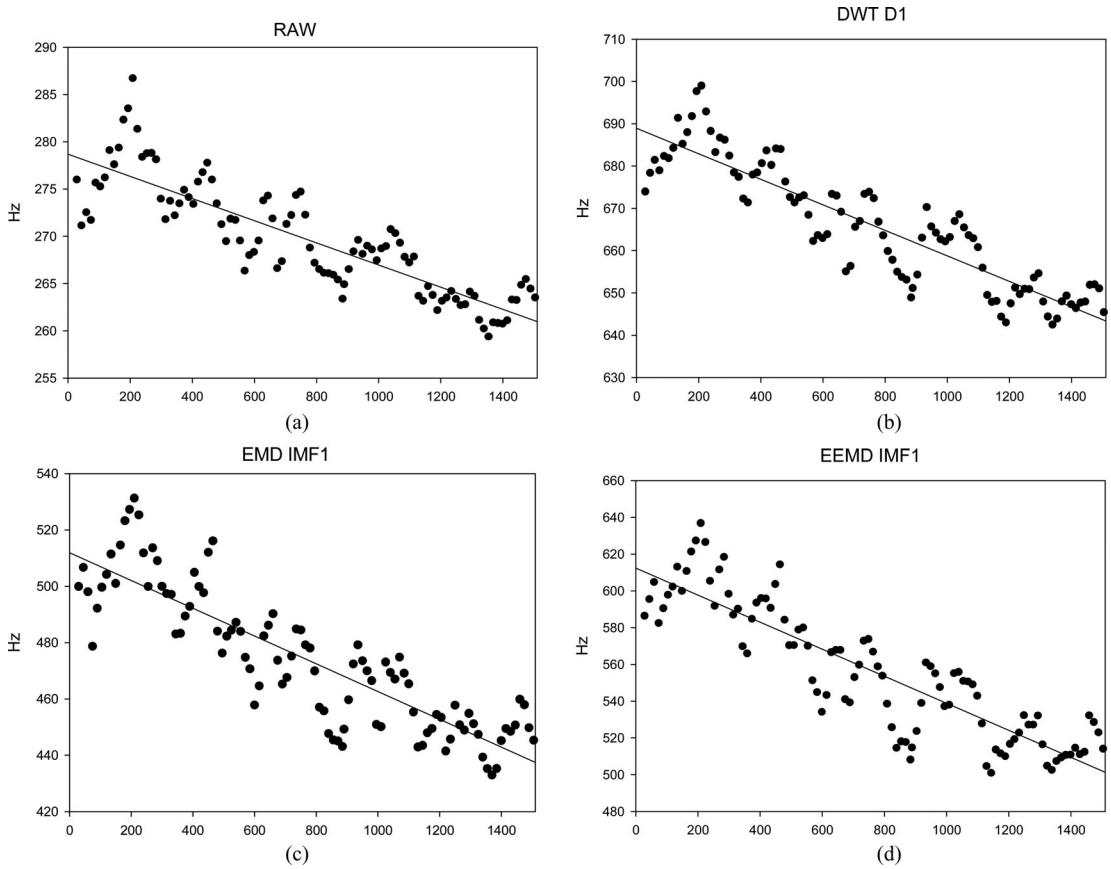

Fig. 8. MF distributions of the raw data, the $D1$ component of the DWT, and the IMF1 components of the EMD and EEMD.

TABLE II
TYPICAL REGRESSION RESULTS FOR THE RAW DATA AND THE DECOMPOSED SIGNALS OF THE DWT, EMD, AND EEMD FOR ONE SUBJECT

		Slope Hz/sec (A)	Coefficient (R)	MF (Hz)
Raw		-0.012	0.859	269.6 (5.8)
DWT	D1	**-0.030**	0.894	665.7 (14.5)
	D2	-0.001	0.365	344.6 (1.4)
	D3	-0.001	0.218	184.6 (1.3)
	D4	-0.000	0.044	107.8 (0.7)
	D5	-0.000	0.094	56.5 (0.4)
	A5	-0.000	0.302	0.03 (0.0)
EMD	IMF1	**-0.049**	0.865	474.0 (24.5)
	IMF2	-0.025	0.874	269.7 (12.4)
	IMF3	-0.010	0.813	167.7 (5.1)
	IMF4	-0.006	0.838	118.8 (2.8)
	IMF5	-0.005	0.904	88.8 (2.5)
	IMF6	-0.005	0.824	65.9 (2.5)
EEMD	IMF1	**-0.074**	0.879	555.8 (36.0)
	IMF2	-0.026	0.877	294.9 (13.0)
	IMF3	-0.011	0.844	178.7 (5.7)
	IMF4	-0.006	0.880	123.5 (2.7)
	IMF5	-0.005	0.904	92.5 (2.2)
	IMF6	-0.011	0.844	69.5 (2.1)

The most significant slope stage for each method is marked in bold.
The MF is represented as the mean (SD).
SD is standard deviation.

TABLE III
STATISTICAL RESULTS OF THE MF SLOPE OF THE RAW DATA AND THE DECOMPOSITION METHODS WITHIN THE THREE LEVELS AND FOR THE ENTIRE EXPERIMENT

Level	RAW (n=60)	DWT (n=60)	EMD (n=60)	EEMD (n=60)
L2	-0.0164*** (0.0144)	-0.0232*** (0.0176)	-0.0456* (0.0356)	**-0.0640 (0.0423)**
L4	-0.0125*** (0.0100)	-0.0209*** (0.0157)	-0.0362* (0.0302)	**-0.0524 (0.0385)**
L6	-0.0193*** (0.0154)	-0.0276*** (0.0264)	-0.0501 (0.0503)	**-0.0687 (0.0636)**
All	-0.0197*** (0.0128)	-0.0296*** (0.0153)	-0.0594** (0.0364)	**-0.0813 (0.0365)**

SD is standard deviation, ALL represents the entire exercise, p<0.05*; p<0.01**; p<0.001**.

muscle fatigue. The studied results of Bonato showed that the CWD was the most suitable method to represent the nonstationary EMG signal during dynamic contraction. However, the use of the CWD requires careful selection of the parameters in the kernel. Moreover, the signal-to-noise ratio also is a critical problem in these analyses, which limits the upper frequency when calculating for the time-dependent mean or MF [31].

Although electrical manifestation of muscle fatigue could be represented by many parameters during a continuous dynamic contraction, these analyzing methods all have to adjust their

TABLE IV
STATISTICAL RESULTS OF THE MF SLOPE OF THE RAW DATA AND THE DECOMPOSITION METHODS DURING THE ENTIRE EXERCISE AT THE SIX MEASUREMENTS

	First (n=10)	Second (n=10)	Third (n=10)	Fourth (n=10)	Fifth (n=10)	Sixth (n=10)
RAW	-0.0181 (0.0125)	-0.0164 (0.010)	-0.0237 (0.0150)	-0.0193 (0.0137)	-0.0201 (0.0147)	-0.0206 (0.0124)
DWT	-0.0290 (0.0154)	-0.0274 (0.0151)	-0.0338 (0.0144)	-0.0283 (0.0169)	-0.0298 (0.0153)	-0.0292 (0.0177)
EMD	-0.0559 (0.0328)	-0.0530 (0.0319)	-0.0713 (0.0380)	-0.0547 (0.0420)	-0.0583 (0.0343)	-0.0629 (0.0439)
EEMD	**-0.0782 (0.0324)**	**-0.0772 (0.0375)**	**-0.0903 (0.0340)**	**-0.0772 (0.0396)**	**-0.0845 (0.0364)**	**-0.0805 (0.0453)**

SD is the standard deviation

TABLE V
STATISTICAL RESULTS OF THE SLOPE COV OF THE RAW DATA AND THE DECOMPOSITION METHODS WITHIN THE THREE LEVELS AND FOR THE ENTIRE EXPERIMENT

Level	RAW (n=10)	DWT (n=10)	EMD (n=10)	EEMD (n=10)
L2	0.7348 (0.2831)	0.6394 (0.2411)	0.7254 (0.2398)	**0.5887 (0.3063)**
L4	0.4791 (0.1922)	0.5611 (0.2874)	0.5326 (0.2613)	**0.5203 (0.2592)**
L6	0.6805 (0.2548)	0.7927 (0.2784)	0.8005 (0.3181)	**0.7195 (0.3603)**
All	0.3689 (0.2159)	0.3156 (0.1984)	0.4000 (0.1905)	**0.2500 (0.1409)**

SD is the standard deviation, ALL represents the entire experiment.

TABLE VI
STATISTICAL RESULTS OF THE MF CORRELATION COEFFICIENT OF THE RAW DATA AND THE DECOMPOSITION METHODS WITHIN THE THREE LEVELS AND FOR THE ENTIRE EXPERIMENT

Level	RAW (n=60)	DWT (n=60)	EMD (n=60)	EEMD (n=60)
L2	0.5136 (0.2727)	0.5496 (0.2687)	0.4996 (0.2704)	**0.5867 (0.2734)**
L4	0.5647 (0.2330)	0.5525 (0.2679)	0.5067 (0.2533)	**0.5771 (0.2692)**
L6	0.5737 (0.2554)	0.5185 (0.2672)	0.4350 (0.2532)	**0.5122 (0.2729)**
All	0.8200* (0.1852)	0.8279 (0.1677)	0.8158* (0.1744)	**0.8763 (0.1022)**

SD is the standard deviation, ALL represents the entire experiment, p<0.05*; p<0.01**; p<0.001***.

TABLE VII
STATISTICAL RESULTS OF THE CORRELATION COEFFICIENT COV OF THE RAW DATA AND THE DECOMPOSITION METHODS WITHIN THE THREE LEVELS AND FOR THE ENTIRE EXPERIMENT

Level	RAW (n=10)	DWT (n=10)	EMD (n=10)	EEMD (n=10)
L2	0.4867 (0.2212)	0.4487 (0.2129)	0.5346 (0.256)	**0.4082 (0.2858)**
L4	0.3426 (0.1793)	0.3807 (0.1985)	0.3816 (0.2289)	**0.3855 (0.3062)**
L6	0.4229 (0.1904)	0.5348 (0.1142)	0.5742 (0.2372)	**0.5073 (0.3208)**
All	0.1608 (0.1810)	0.1309 (0.1426)	0.1500 (0.1473)	**0.0716 (0.0732)**

SD is the standard deviation, ALL represents the entire experiment.

parameters on a case-by-case basis. Moreover, monitoring the electrical manifestations of muscle fatigue during the dynamic contraction is better useful than the static contraction in the real life. Therefore, in this study, the goal was not to quantify the electrical manifestation of muscle fatigue. Our goal is to find a more sensitive and stable method to sense the progression of muscle fatigue in the local muscle during the exercise.

Also, the frequency range of sEMG is defined within 100 to 500 Hz in an isometric contraction. In this study, because we considered the nonstationary characteristics of the dynamic sEMG, we increased the measured bandwidth for the decomposed analyses. The sampling rate was raised to 2000 Hz. Moreover, because the maximum speed of the experiment is about 100 SPM, the artifact noises, produced by electrode movement, the shift of muscle, and the change of innovation zone, all belong to the low-frequency component [32]. In Fig. 4, the low-frequency energy of the raw sEMG is significantly larger than the high-frequency energy. We used the decomposed methods to filter the low-frequency component of the raw sEMG signal. The highest frequency components to sense the progression of muscle fatigue have a better sensitivity than the raw sEMG in Table III.

In these decomposed methods, EMD acted as a filter bank, and there was no strict bandwidth restriction with the IMF. The frequency range of each IMF level is adaptive, depending on the raw signal content. Therefore, in Fig. 6, the IMF1 of EMD also has the low-frequency energy. Comparing the IMF components of the same level, EEMD is more concentrated and has band-limited components. With the iterative EMD computation, the average of each IMF scale yielded a sharper band transition than a single EMD-derived IMF. The transition band overlap between adjacent IMFs is reduced. EEMD acts as a higher order filter with the same filter specification as EMD with a lower filter order. IMF mode mixing reduction is the major advantage of EEMD over EMD. Thus, in Table II, the average MF of the IMF1 component of EEMD is larger than that of the EMD, and the MF slope of the IMF1 of EEMD is sharper than that of the EMD.

The DWT decomposition is based on the successive filtering of the symmetric half-band high-pass and low-pass filters. The frequency range of the more detailed component is nearly twice that of the adjacent less detailed component. In Table II, although the MF of the $D1$ component of DWT is largest than the IMF1 component of EMD and EEMD, the absolute MF slope of the IMF1 component of EEMD is largest during the entire exercise. In Table III, the absolute MF slope of the IMF1 component of EEMD is also largest and has the significant difference with the raw sEMG signal and the highest frequency component of DWT and EMD.

Because the subjects easily stepped the elliptical trainer during level $L2$, the signal-to-noise ratio of sEMG signal is lower than the other levels. Thus, in Table III, all absolute MF slopes in level $L2$ are larger than those of level $L4$. However, the slope CoVs in level $L2$ is larger than the level $L4$ in Table V. The subjects hardly stepped on the elliptical trainer during level $L6$. The signal-to noise ratio of the sEMG signal is larger than the other levels. The absolute MF slopes in level $L6$ are largest. These

results show that the signal-to-noise ratio of the sEMG signal during the dynamic contraction will affect the manifestation of muscle fatigue [32].

In Table VI, although the correlation coefficient of the MF1 of EEMD only has the significant difference for the raw sEMG signal and EMD during the entire exercise, its value is largest in levels $L2$, $L4$, and the entire exercise. However, in level $L6$, this phenomenon is not true. The reason for this is that the subjects may be running their maximum in level $L6$ until they cannot run. Thus, the difference of every subject is very large. However, if the entire exercise was considered, the IMF1 of EEMD has the better consistency for sensing the progression of muscle fatigue.

In the repeatable test, the means and standard deviations of the absolute slope and correlation coefficient CoVs of the MF of the IMF1 of the EEMD method all are the smallest values than the raw sEMG signal and the other decomposed methods during the entire exercise. That is, the MF of the IMF1 of the EEMD method sensed the progression of muscle fatigue being more stable than with the raw sEMG signal and the highest frequency components of other decomposed methods.

Finally, we had done two hypotheses in Section I. The first hypothesis was that healthy subjects run a fixed speed with the different loads in muscle activity as fatigue progressed. In Fig. 8, we see that the MF of the raw data, the $D1$ component of the DWT, and the IMF1 components of the EMD and the EEMD all shift to the lower frequency. This result proved our first hypothesis. Our second hypothesis was that the spectral parameters of sEMG have a significant change during the dynamic contraction when the decomposed signal of sEMG reduced the nonstationary characteristics and noise. In Table III, the absolute MF slope of the highest frequency component of DWT, EMD, and EEMD are all larger than the raw sEMG during the three loading levels and the entire exercise. This result also proved our second hypothesis.

The fact that the EMG spectrum scales toward the lower frequencies as muscle contraction is sustained is very well known. Therefore, it is clear that the upper frequencies are the most important to quantify muscle fatigue. In this study, we used the DWT, EMD, and EEMD to decompose the raw sEMG. The results show that the highest frequency component of the sEMG signal for sensing the progression of muscle fatigue has higher sensitivity and consistency than the raw sEMG signal or the low-frequency component of the sEMG signal. The performance of the highest frequency component by the EEMD method is better than the DWT and EMD methods.

REFERENCES

[1] A. Kaikkonen, A. Natri, M. Pasanen, K. Latvala, P. Kannus, and M. Jarvinen, "Isokinetic muscle performance after surgery of the lateral ligaments of the ankle," *Int. J. Sports Med.*, vol. 20, no. 3, pp. 173–178, Apr. 1999.

[2] T. Mittlmeier, A. Weiler, T. Sohn, L. Kleinhans, S. Mollbach, G. Duda, and N. P. Sudkamp, "Novel award second prize paper: Functional monitoring during rehabilitation following anterior cruciate ligament reconstruction," *Clin. Biomech.*, vol. 14, no. 8, pp. 576–584, Oct. 1999.

[3] A. Beelen and A. J. Sargeant, "Effect of fatigue on maximal power output at different contraction velocities in humans," *J. Appl. Physiol.*, vol. 71, no. 6, pp. 2332–2337, Dec. 1991.

[4] A. St Clair Gibson, M. I. Lambert, J. J. Durandt, N. Scales, and T. D. Noakes, "Quadriceps and hamstrings peak torque ratio changes in persons with chronic anterior cruciate ligament deficiency," *J. Orthop. Sports Phys. Ther.*, vol. 30, no. 7, pp. 418–427, Jul. 2000.

[5] S. L. Morris and G. T. Allison, "Effects of abdominal muscle fatigue on anticipatory postural adjustments associated with arm raising," *Gait Posture*, vol. 24, no. 3, pp. 342–348, Nov. 2006.

[6] L. R. Brody, M. T. Pollock, S. H. Roy, C. J. De Luca, and B. Celli, "pH-induced effects on median frequency and conduction velocity of the myoelectric signal," *J. Appl. Physiol.*, vol. 71, no. 5, pp. 1878–1885, Nov. 1991.

[7] C. J. De Luca, "Myoelectrical manifestations of localized muscular fatigue in humans," *Crit. Rev. Biomed. Eng.*, vol. 11, no. 4, pp. 251–279, 1984.

[8] R. Merletti, M. Knaflitz, and C. J. De Luca, "Myoelectric manifestations of fatigue in voluntary and electrically elicited contractions," *J. Appl. Physiol.*, vol. 69, no. 5, pp. 1810–1820, Nov. 1990.

[9] E. A. Froese and M. E. Houston, "Torque-velocity characteristics and muscle fiber type in human vastus lateralis," *J. Appl. Physiol.*, vol. 59, no. 2, pp. 309–314, Aug. 1985.

[10] E. J. Kupa, S. H. Roy, S. C. Kandarian, and C. J. De Luca, "Effects of muscle fiber type and size on EMG median frequency and conduction velocity," *J. Appl. Physiol.*, vol. 79, no. 1, pp. 23–32, Jul. 1995.

[11] J. V. Basmajian and C. J. DeLuca, *Muscles Alive: Their Functions Revealed by Electromyography*. Baltimore, MD: Williams & Wilkins, 1985, p. 561.

[12] D. Farina, R. Merletti, M. Nazzaro, and I. Caruso, "Effect of joint angle on EMG variables in leg and thigh muscles," *IEEE Eng. Med. Biol. Mag.*, vol. 20, no. 6, pp. 62–71, Nov./Dec. 2001.

[13] F. Molinari, M. Knaflitz, P. Bonato, and M. V. Actis, "Electrical manifestations of muscle fatigue during concentric and eccentric isokinetic knee flexion-extension movements," *IEEE Trans. Biomed. Eng.*, vol. 53, no. 7, pp. 1309–1316, Jul. 2006.

[14] M. Knaflitz and F. Molinari, "Assessment of muscle fatigue during biking," *IEEE Trans. Neural Syst. Rehabil. Eng.*, vol. 11, no. 1, pp. 17–23, Mar. 2003.

[15] J. B. Dingwell, J. E. Joubert, F. Diefenthaeler, and J. D. Trinity, J. E. Joubert, F. Diefenthaeler *et al.*, "Changes in muscle activity and kinematics of highly trained cyclists during fatigue," *IEEE Trans. Biomed. Eng.*, vol. 55, no. 11, pp. 2666–2674, Nov. 2008.

[16] V. von Tscharner, "Time-frequency and principal-component methods for the analysis of EMGs recorded during a mildly fatiguing exercise on a cycle ergometer," *J. Electromyogr. Kinesiol.*, vol. 12, no. 6, pp. 479–492, Dec. 2002.

[17] M. Talebinejad, A. D. Chan, and A. Miri, "A Lempel–Ziv complexity measure for muscle fatigue estimation," *J. Electromyogr. Kinesiol.*, vol. 21, no. 2, pp. 236–241, Apr. 2011.

[18] H. B. Xie, J. Y. Guo, and Y. P. Zheng, "Fuzzy approximate entropy analysis of chaotic and natural complex systems: Detecting muscle fatigue using electromyography signals," *Ann. Biomed. Eng.*, vol. 38, no. 4, pp. 1483–1496, Apr. 2010.

[19] M. Gonzalez-Izal, A. Malanda, E. Gorostiaga, and M. Izquierdo, "Electromyographic models to assess muscle fatigue," *J. Electromyogr. Kinesiol.*, vol. 22, no. 4, pp. 501–512, Aug. 2012.

[20] N. E. Huang, Z. Shen, S. R. Long, M. C. Wu, H. H. Shih, Q. Zheng, N.-C. Yen, C. C. Tung, and H. H. Liu, "The empirical mode decomposition and the Hilbert spectrum for nonlinear and non-stationary time series analysis," *Phys. Eng. Sci.*, vol. 454, no. 1971, pp. 903–996, 1998.

[21] M. Hassan, S. Boudaoud, J. Terrien, B. Karlsson, and C. Marque, "Combination of canonical correlation analysis and empirical mode decomposition applied to denoising the labor electrohysterogram," *IEEE Trans. Biomed. Eng.*, vol. 58, no. 9, pp. 2441–2447, Sep. 2011.

[22] A. Karagiannis and P. Constantinou, "Noise-assisted data processing with empirical mode decomposition in biomedical signals," *IEEE Trans. Inf. Technol. Biomed.*, vol. 15, no. 1, pp. 11–18, Jan. 2011.

[23] V. Srhoj-Egekher, M. Cifrek, and V. Medved, "The application of Hilbert–Huang transform in the analysis of muscle fatigue during cyclic dynamic contractions," *Med. Biol. Eng. Comput.*, vol. 49, no. 6, pp. 659–669, Jun. 2011.

[24] W. Zhaohua, E. Norden, and Huang, "Ensemble empirical mode decomposition: a noise-assisted data analysis method," *Adv. Adaptive Data Anal.*, vol. 1, no. 1, pp. 1–41, 2009.

[25] A. Rainoldi, M. Nazzaro, R. Merletti, D. Farina, I. Caruso, and S. Gaudenti, "Geometrical factors in surface EMG of the vastus medialis and lateralis muscles," *J. Electromyogr. Kinesiol.*, vol. 10, no. 5, pp. 327–336, Oct. 2000.

[26] F. B. Stulen and C. J. DeLuca, "Frequency parameters of the myoelectric signal as a measure of muscle conduction velocity," *IEEE Trans. Biomed. Eng.*, vol. BE-28, no. 7, pp. 515–523, Jul. 1981.

[27] H. Xie and Z. Wang, "Mean frequency derived via Hilbert–Huang transform with application to fatigue EMG signal analysis," *Comput. Methods Programs Biomed.*, vol. 82, no. 2, pp. 114–120, May 2006.
[28] B. Hannaford and S. Lehman, "Short time fourier analysis of the electromyogram: Fast movements and constant contraction," *IEEE Trans. Biomed. Eng.*, vol. BE-33, no. 12, pp. 1173–1181, Dec. 1986.
[29] S. Karlsson and B. Gerdle, "Mean frequency and signal amplitude of the surface EMG of the quadriceps muscles increase with increasing torque—A study using the continuous wavelet transform," *J. Electromyogr. Kinesiol.*, vol. 11, no. 2, pp. 131–140, Apr. 2001.
[30] G. Gagliati and M. Knaflitz, "Analysis of myoelectric signals recorded during dynamic contractions," *IEEE Eng. Med. Biol. Mag.*, vol. 15, no. 6, pp. 102–111, 1996.
[31] P. Bonato, S. H. Roy, M. Knaflitz, and C. J. De Luca, "Time-frequency parameters of the surface myoelectric signal for assessing muscle fatigue during cyclic dynamic contractions," *IEEE Trans. Biomed. Eng.*, vol. 48, no. 7, pp. 745–753, Jul. 2001.
[32] R. Merletti and P. Parker, *Electromyography: Physiology, Engineering, and Noninvasive Applications*. Hoboken, NJ: Wiley, 2004.

Shing-Hong Liu received the B.S. degree in electronic engineering from Feng-Jia University, Taizhon, Taiwan, R.O.C., in 1990, the M.S. degree in biomedical engineering from the National Cheng-Kung University, Tainan, Taiwan, R.O.C., in 1992, and the Ph.D. degree from the Department of Electrical and Control Engineering, National Chiao-Tung University, Hsinchu, Taiwan, R.O.C., in 2002.

August 1994, he has been a Lecturer in the Department of Biomedical Engineering, Yuanpei University, Hsinchu, Taiwan, and is an Associate Professor from 2002 to 2008. Now, he is an Professor in the Department of Computer Science and Information Engineering, Chaoyang University of Technology. His current research interests are digital signal processing, fuzzy control and designing biomedical instrument.

Kang-Ming Chang received the Ph.D. degree from the Department of Electrical and Control Engineering, National Chiao-Tung University, Hsinchu, Taiwan, R.O.C., in 2005.

He was an Assistant Professor from 2005 to 2011 in the Department of Photonics and Communication Engineering, Asia University, Taichung, Taiwan. Now, he is an Associate Professor from 2011. His current research interests include biomedical signal processing, especially on stress reduction related issue, either by HRV and brain activity.

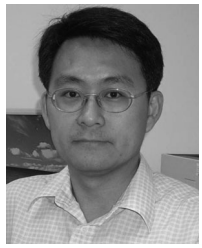

Da-Chuan Cheng received the B.S. degree in electrical engineering from Chinese Culture University, Taiwan, and the M.S. and Ph.D. degrees in biomedical engineering from National Cheng Kung University, Taiwan.

He was a post doctorat at the Department of Mathematics and Computer Science, Westfaelische Wilhelms University Muenster, Germany. Since 2011, he is an Associate Professor at the Department of Biomedical Imaging and Radiological Science of the China Medical University, Taiwan. His research interests include medical image processing and pattern recognition.